



### **Science Arts & Métiers (SAM)**

is an open access repository that collects the work of Arts et Métiers Institute of Technology researchers and makes it freely available over the web where possible.

This is an author-deposited version published in: <https://sam.ensam.eu>  
Handle ID: <http://hdl.handle.net/10985/10823>

#### **To cite this version :**

C. STOLZ, A. MATHIEU, O. AUBRETON, Nicolas CONIGLIO - Real time polarization imaging of weld pool surfaces - In: International Conference on Quality Control by Artificial Vision 2015, 953402 (12;April; , 2015), France, 2015-04 - Twelfth International Conference on Quality Control by Artificial Vision - 2015

Any correspondence concerning this service should be sent to the repository

Administrator : [scienceouverte@ensam.eu](mailto:scienceouverte@ensam.eu)



# *Real time polarization imaging of weld pool surface*

C. Stolz<sup>1</sup>, N. Coniglio<sup>2</sup>, A. Mathieu<sup>3</sup>, and O. Aubreton<sup>1</sup>

<sup>1</sup> Laboratoire Le2i, UMR 6306 CNRS-Université de Bourgogne, 21000, Dijon, France.

<sup>2</sup> Laboratoire MSMP, Arts et Métiers Paris Tech, 13100 Aix en Provence, France

<sup>3</sup> Laboratoire ICB, UMR 6303 CNRS-Université de Bourgogne, 71200, Le Creusot, France.

E-mail: [christophe.Stolz@u-bourgogne.fr](mailto:christophe.Stolz@u-bourgogne.fr)

## ABSTRACT

The search for an efficient on-line monitoring system focused on the real-time analysis of arc welding quality is an active area of research. The topography and the superficial temperature field of the weld pool can provide important information which can be used to regulate the welding parameters for depositing consistent welds. One difficulty relies on accessing this information despite the bright dazzling welding arc. In the present work, Stokes polarimetry and associated shape-from-polarization methods are applied for the analysis of the weld pool through its 810 nm-wavelength infrared emissions. The obtained information can provide a better understanding of the process, such as the usage of the topography to seek Marangoni flows direction, or to have a denser 3D map to improve numerical simulation models.

**Keywords:** Stokes polarimetry, polarimetric imaging, three dimensional sensing.

## 1. INTRODUCTION

Topographic characterizations of metallic weld pool surfaces are required for a better quality control. For example, the weld pool concavity/convexity informs about the lack/excess of filler metal. Defect formation must be minimized during the processing stage to ensure efficient, high-quality production. The quality of deposited welds usually requires the knowledge of the physical behavior of the welding process. The superficial temperature field of the weld pool provides important information on its behavior from viewpoints of both fluid dynamics, solidified microstructure, and, consequently, mechanical properties of the joint. An interest to develop sensors is growing in order to provide accurate, robust, real-time monitoring of these thermal characteristics. The corresponding experimental estimation may also be useful for improving the actual models used during simulations of the welding process.

Topographic measurement of specular surfaces imposes the use of specific techniques [1], among which only a few have been applied to welding conditions [2-4]. Techniques using laser pattern projection and shape-from distortion approaches, require a particular coding of the pattern, difficult to recognize when the concavity changes. Figure 1 shows an example of pattern reflected by the surface of the weld pool during a stationary Gas Tungsten Arc (GTA) experiment. At the contrary, shape-from-polarization methodologies provide a dense reconstruction of uncontaminated surfaces without ambiguity on the weld pool concavity and the thermal field from a same single measurement. Shape-from-polarization methodology applied to thermal radiation emitted by a weld pool surface estimates the surface orientation from the polarimetric state of the emitted light, and subsequently provides a discrete gradient vector field for a discrete set of radiating points on object surfaces. The polarimetry of thermal emissions requires no external illumination and can deduce surface normals without ambiguous  $\theta$  values as the  $\rho$ - $\theta$  relationship for thermal emissions is a bijective monotonically-increasing relationship [5-7]. Thermal emissions are infrared body emissions partially linearly polarized in the far field [8] in a direction parallel to the plane of incidence for objects large compared to the emitted wavelength. The dependencies of their polarization state upon surface condition [9] and emergence angle  $\alpha$  have been observed for various materials, such as metallic surfaces [10]. Thus the polarized state of thermal radiations contains geometrical information of the emitting surface. In this paper, we get these properties associated with a high speed camera in order to acquire dynamic of the weld pool.

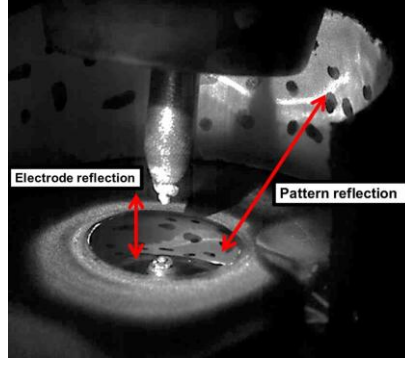


Figure 1. Stationary GTA welding of steel using helium shielding gas observed during welding performance using an external Cavilux laser lighting (810 nm wavelength). The arc plasma is transparent at this wavelength.

## 2. METHODOLOGY

The polarimetric analysis of the emitted radiations from the scene is done by using the Stokes model. Three ( $S_0$ ,  $S_1$ ,  $S_2$ ) out of the four unknown Stokes parameters of the thermal radiations are determined by interpolating the equation for each corresponding pixel in each sub-image of a linear polarizer at an angle  $\alpha$  [11,12].

$$\begin{cases} I(\alpha) = \frac{1}{2} \times (S_0 + S_1 \times \cos(2\alpha) + S_2 \times \sin(2\alpha)) \\ I(\alpha) = \frac{1}{2} \times (1 + \rho \times \cos(2\alpha - 2\varphi)) \end{cases} \quad \text{with} \quad \rho = \frac{\sqrt{S_1^2 + S_2^2}}{S_0} \quad (1)$$

where  $\rho(u,v)$  is degree of linear polarization (DOLP),  $I(u,v)$  is light magnitude, and  $\varphi(u,v)$  is angle of polarization (AOP) at each pixel of image coordinates  $(u,v)$ . As thermal emissions are partially linearly polarized parallel to the plane of incidence, the azimuthal angle  $\phi$  is related to  $\varphi$  by:

$$\phi = \varphi - (\text{sgn}(S_1) + 1) \times \frac{\pi}{2} = \frac{1}{2} \times \arctan\left(\frac{S_2}{S_1}\right) - (\text{sgn}(S_1) + 1) \times \frac{\pi}{2} \quad (2)$$

where  $\text{sgn}()$  is the signum function. The total emissivity  $\varepsilon$  of thermal emissions is the mean value of the emissivities  $\varepsilon_{//}$  and  $\varepsilon_{\perp}$  of thermal emissions with a polarization direction parallel and perpendicular to the plane of incidence, respectively. The emergence angle  $\theta$  is then inferred using the bijective relation [7]:

$$\rho = \left( \frac{\varepsilon_{//} - \varepsilon_{\perp}}{\varepsilon_{//} + \varepsilon_{\perp}} \right) = \frac{(n^2 + k^2 - 1) \times (1 - \cos^2 \theta)}{(1 + n^2 + k^2) \times (1 + \cos^2 \theta) + 4n \times \cos \theta} \quad (3)$$

The refractive index,  $n - ik = 8 - 2.3i$  [13], is used for the surface reconstruction. Once the emissivity of a radiated point is calculated, the point temperature  $T$  is deduced from a calibrated relationship between the measured intensity  $S_0$  and the radiance of a blackbody at a known temperature according to Planck's law. Hence the polarimetric state of radiated light permits both thermal field and topographic reconstruction, using [14]. Figure 2 details the steps of the algorithm.

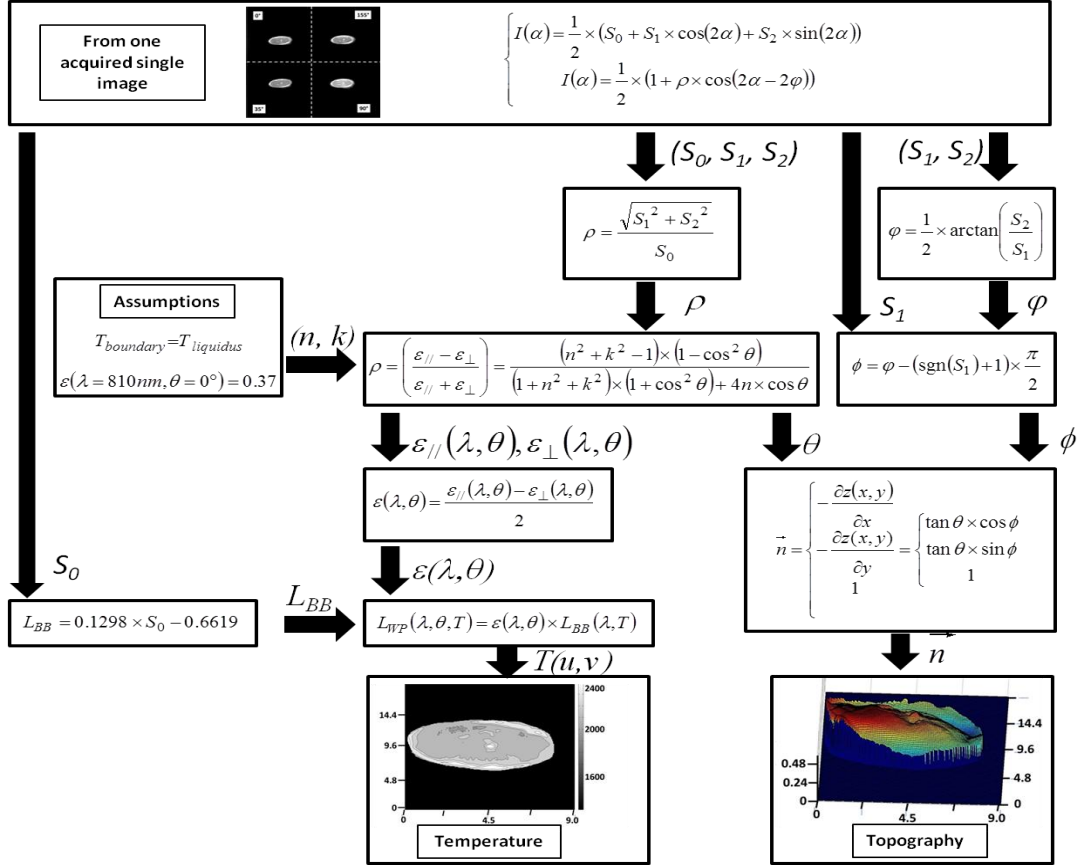


Figure 2. Schematic view of the methodology to recover 3D surface topography and surface thermal field.

First, extraction of the four polarization images is performed and Stokes parameters are extracted, involving the estimation of the degree and angle of polarization. From the assumption that the temperature of the liquidus is approximately the one of the boundary of the weld pool, the refractive index is estimated and include in the emissivity relationships. The temperature map and the topography are finally evaluated.

The feasibility of the method for extraction of topography was recently proven on stationary Gas Tungsten Arc (GTA) welds[13]. The 810 nm-wavelength chosen for observation corresponded to a blind spectral window of the helium shielding gas plasma. In this paper we present experiments including the temperature maps.

### 3. RECENT EXPERIMENTS

We have implemented our approach by using a monospectral near-infrared polarimeter. The weld pool is observed by a Phantom V9.1 camera at a grazing angle of  $23^\circ$  through a 810 nm narrow bandpass filter during welding. Fitted on the Phantom V9.1 camera, a wavefront division polarimetric system [15] (MultiSpec imager) is equipped with four Polarcor linear polarizers 05P109AR.16 from Newport to make simultaneously all polarization measurements for every pixel of the dynamic scene (Figure 3). The camera CMOS (complementary metal-oxide-semiconductor) sensor allows for short exposure durations, which are necessary to observe dynamic scenes. Images are acquired at 500 Hz frequency. An aperture f/2.8 and exposure time 300  $\mu\text{s}$  are selected. An extension ring was also mounted on the lens in order to improve the resolution on the weld pool. Calibration of the system was required to analyze quantitatively the emission. Prior to DOLP and AOP calculations, the pixel-to-pixel matching between the four sub-images is made using X-Y translation of each sub-image of a grid pattern. Due to the multiSpec imager optical design, no sub-image rotation is needed. The relative grey-level attenuation coefficient of each light path was evaluated by acquiring an image without polarized filters and applied on the corresponding polarized sub-image. The object radiance  $L$  ( $\text{W} \times \text{sr}^{-1} \times \text{m}^{-2} \times \text{nm}^{-1}$ ), calculated with Planck's law, was associated to the Stokes parameter  $S_0$  by filming a heated blackbody made in ceramic  $\text{LaCrO}_3$  from 473 to 1923 K inside a pyrometer calibration furnace Pyrox PY15.

$$\text{LBB of fig 1 } L = 0.1298 \times S_0 - 0.6619 \quad (4)$$

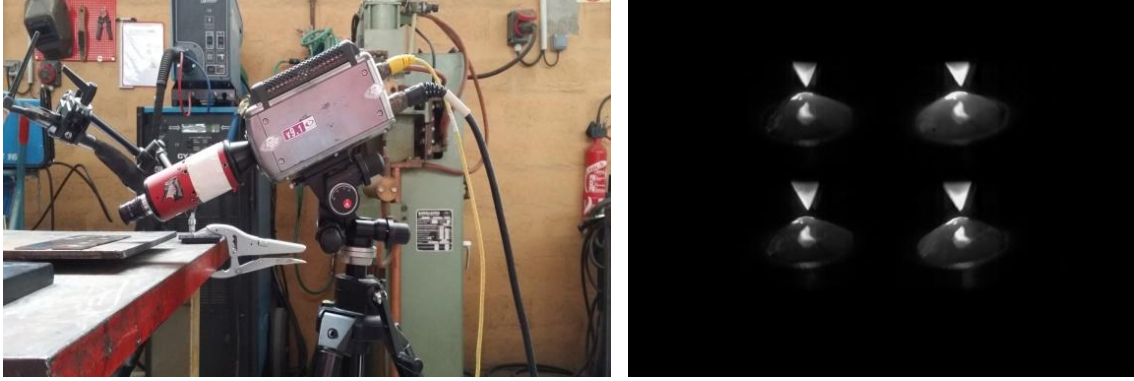


Figure 3 : a) Experience of GTAW welding on steel b) One shot of the acquired sequence showing the weld pool in the four polarization orientations.

We have filmed during 3 seconds, the weld pool, in static conditions, on a low carbon steel plate. The welding conditions were as follows: 80A DCEN (Direct Current Electrode Negative) polarity with a flow rate of Helium set to 10 L/min. The choice of this shielding gas is due to the low emission of the generated plasma at the working wavelength. We repeated the experience several times in order to have stable conditions. Indeed, in one of the sequence we observe a modification of the shape of the weld pool. The surface was growing into the direction of the tungsten tip (Figure 4d) during one of these shot, may be due to some movements during the experiment. We have processed a part of the sequence. Three instants, at 1.03, 1.13, and 1.3 seconds, before and onto the growing of the weld pool are showed on Figure 3 in order to illustrate the evolution of the changes of the weld pool during the time interval where the current is switched on. In each case, the temperature map is also estimated. The estimation of the degree of polarization is also showed. Notice that denoising operator is applied to each subimage before the DOP estimation and that the region of interest is the weld pool itself. The screenshots clearly shows that the static point on the top of the weld pool may correspond either to some oxide particle that emits intensively at the working wavelength, or to the reflection of the tungsten tip on the weld pool surface.

Weld pool surface topography should be influenced by two factors. First factor, the solid-liquid state transformation is accompanied by a volume increase and leads to a mean surface level above the flat workpiece surface level. Second factor, surface convexity or concavity may be induced by the liquid surface tension and/or arc pressure. Surface tension gradient give birth to strong liquid flow called Marangoni convection. Liquid flows from the boundary region to the center of the weld pool are observed with both the oxide particles movement from the boundary to the center of the weld pool and with the liquid metal getting hotter when closer to the molten pool edges. The white spot observed in the center of the weld pool is due to an accumulation of these oxide particles. Due to its higher emissivity compared to liquid surface one, oxides emits more intensively at 810 nm wavelength.

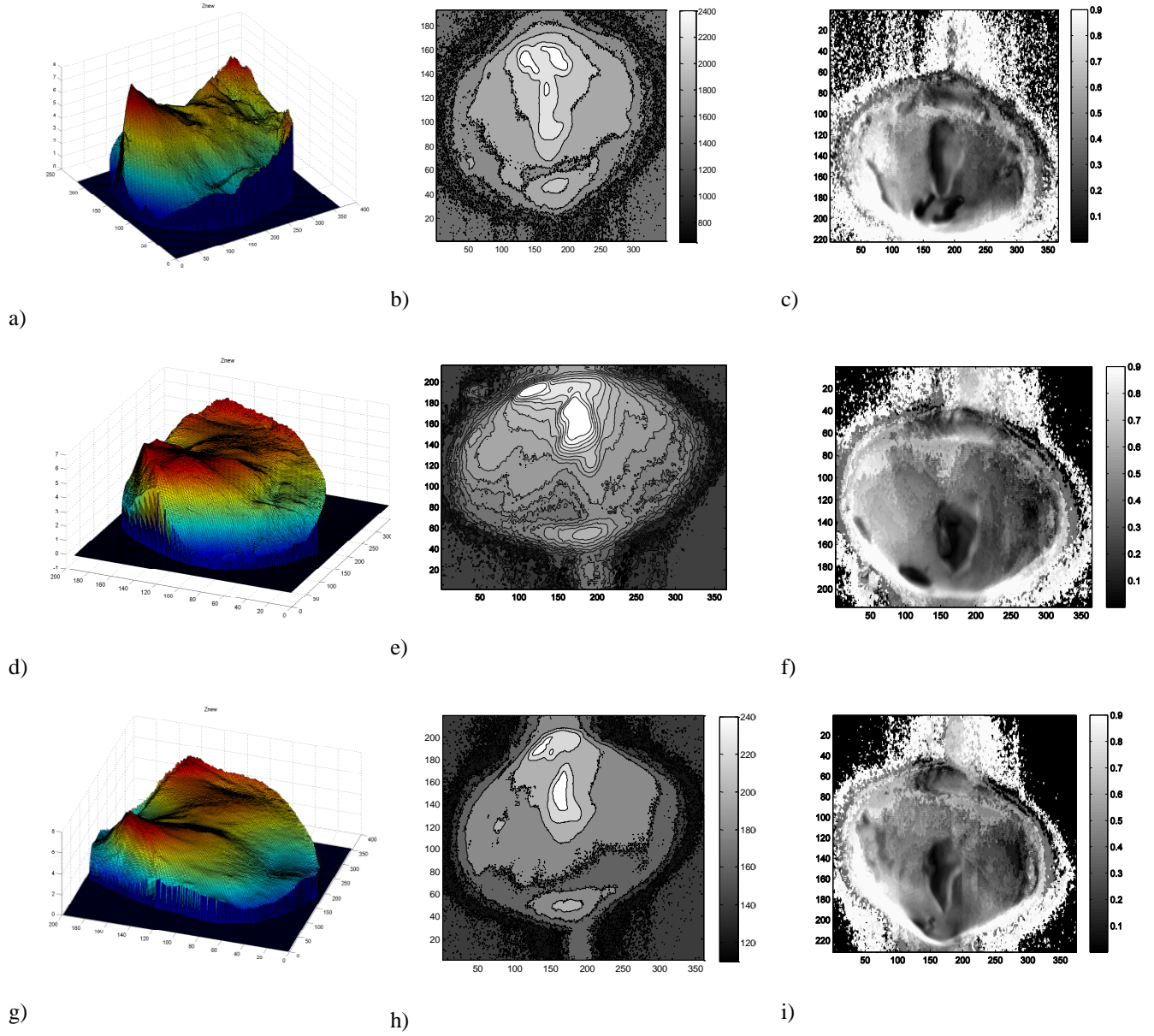


Figure 4: Example of 3D depth estimation, temperature map and degree of polarization for four instants of the processed sequence; a, b and c at 1.03 s; d, e and f at 1.13s; g, h and i at 1.3s

The radiations of these floating oxides saturate the corresponding CMOS pixels, hence estimating the temperature to be over 2400 K. As the saturation effect does not permit a correct estimation of the polarization state of the emitted light, this creates an aberration, such as a hole onto the reconstructed surface center (Figure 3-a) that may possibly not exist on the real surface.

Next steps to improve the method, will be to segment the surface of the weld pool in order to link the segmentation results to the physical parameters involved here.



## 4. CONCLUSION

During this work we studied the polarimetric state of thermal radiations emitted from a weld pool generated by GTA. Stokes polarimetry is a novel method to characterize such a weld pool surface. The shape-from-polarization method applied for a 810 nm-wavelength infrared emission enables the access to dense thermal and topographic information about GTA weld pool surfaces. In this paper we showed the possibility of the method to explore the weld pool during time. Future works will concern a more accurate spectral study in order to find an appropriate working wavelength when traditional Argon shielding gas is used due to its highest density, but the induced plasma is highly emissive for our sensor. We will also study weld pools induced by metal/laser interaction, with a focus on keyhole weld pool surface. For such cases, a methodology should be developed either to move away the iron vapor plume without perturbing the keyhole hydro-dynamics or, more probable, to apply the shape-from-polarization at an infrared wavelength at which iron vapor is transparent. Shape-from-polarization method can also have some extension as a method for determination of complex refractive index ( $n$ ,  $k$ ) in the case of molten metal.

## REFERENCES

- [1] K. Ikeuchi, "Constructing A Depth Map from Images", A.I Memo AIM-744, Artificial Intelligence Laboratory, MIT (1983).
- [2] H.S. Song and Y.M. Zhang, "Three-dimensional reconstruction of specular surface for a gas tungsten arc weld pool ", *Measurement Science and Technology* Vol. 18, pp. 3751-3767, 2007.
- [3] W. Zhang, X. Wang and Y. Zhang, "Analytical real-time measurement of a three-dimensional weld pool surface", *Measurement Science and Technology* Vol. 24 (11), pp. 115011, 2013.
- [4] C. Mnich, F. Al-Bayat, C. Debrunner, J.P.H. Steele and T. Vincent, "In Situ Weld Pool Measurement Using Stereovision", *Japan-USA Symposium on Flexible Automation*, Denver, Colorado, ASME, 2004 Vol., 2004.
- [5] A.G. Worthing, "Deviation from Lambert's and polarization of light emitted by incandescent tungsten, tantalum and molybdenum and changes in the optical constants of tungsten with temperature", *J. Opt. Soc. Am.* Vol. 13, pp. 635-647, 1926.
- [6] D. Miyazaki, M. Saito, Y. Sato and K. Ikeuchi, "Determining Surface Orientations of transparent objects on polarization degrees in visible and infrared wavelength", *J. Opt. Soc. Am. A* Vol. 19 (4), pp. 687-694, 2002.
- [7] K.P. Gurton, R. Dahmani and G. Videen, "Measured Degree of Infrared Polarization for a Variety of Thermal Emitting Surfaces", *ARL-TR* (2004).
- [8] D.C. Bertilone, "Stokes parameters and partial polarization of far-field radiation emitted by hot bodies", *Journal of the Optical Society of America A* Vol. 11 (8), pp. 2298-2304, 1994.
- [9] D.L. Jordan and G. Lewis, "Measurements of the effect of surface roughness on the polarization state of thermally emitted radiation", *Opt. Lett.* Vol. 19 (10), pp. 692-694, 1994.
- [10] A.J. Sievers, "Thermal radiation from metal surfaces", *J. Opt. Soc. Am.* Vol. 68 (11), pp. 1505-1516, 1978.
- [11] L.B. Wolff, "Polarization vision: a new sensory approach to image understanding", *Image and Vision computing* Vol. 15 (2), pp. 81-93, 1997.
- [12] O. Morel, C. Stolz and P. Gorria, "Polarization imaging for 3D inspection of highly reflective metallic objects", *Optics and Spectroscopy* Vol. 101 (1), pp. 15-21, 2006.
- [13] N. Coniglio, A. Mathieu, O. Aubreton and C. Stolz, "Characterizing weld pool surfaces from polarization state of thermal emissions", *Opt. Lett.* Vol. 38 (12), pp. 2086-2088, 2013.
- [14] R. Frankot and R. Chellappa, "A method for enforcing integrability in shape from shading algorithms", *IEEE Trans. Pattern Anal. Mach. Intell.* Vol. 10 (4), pp. 439-451, 1988.
- [15] S.J. Tyo, D.L. Goldstein, D.B. Chenault and J.A. Shaw, "Review of passive imaging polarimetry for remote sensing applications", *Appl. Opt.* Vol. 45 (22), pp. 5453-5469, 2006.